DESIGN OF DRIVE CONTROL SYSTEM FOR SEED DISCHARGER BASED ON FUZZY PID CONTROL

Jiamin SHI[1], Shihao ZHANG[2],, Shouhua REN[3]*

With the rapid development of planting industry in Heilongjiang region, improving the operational efficiency of seeder as well as stabilizing the seeding quality under complex working environment has become the main research trend in agricultural production. Aiming at the problems of leakage and reseeding that are easily produced by mechanical drive sowing, this study takes the Vset air-absorbing corn seeder as the object of research, and designs a fuzzy PID control based corn seeder driver, and selects the XD-37GB3650 DC brushless motor as the driving power source. The practicality and reliability of the system are verified through Simulink motor speed control system simulation experiments, system response time detection tests, and field tests. Simulation experiment show that: based on the fuzzy PID electric drive seed dispenser control system, the system has no overshooting, the regulation time is 0.1s, and there is no obvious oscillation phenomenon after reaching the steady state; the system response time detection test shows that the system has good followability, and it can cope with emergencies during the operation; Field trials indicate that the control system of the electrically driven seed discharger, under a fixed plant spacing, achieves a seed spacing standard deviation of 2.651 and a coefficient of variation of 10.48% at a tractor speed of 4 km/h. At a speed of 8 km/h, the standard deviation is 1.489 with a coefficient of variation of 6.11%. When the tractor speed reaches 12 km/h, the standard deviation is 2.211 with a coefficient of variation of 8.91%. Both the standard deviation and coefficient of variation outperform those of mechanically driven operations and meet the national standards.

Keywords: Brushless DC Motor Control, Seeder, Fuzzy PID control, Control System Simulation

1 Introduction

Heilongjiang planting industry to a variety of food, planting good food for the most important goal, precise control of crop planting density can ensure that each plant to obtain enough growth space and nutrients, can avoid too dense or too sparse situation, to ensure that the plant survival rate and growth status is good so as to improve the yield [1]. The traditional ground wheel drive and chain drive in

[1] Faculty of Agricultural Engineering and Information Technology, Heilongjiang Bayi Agricultural University, 5 Xin Feng Street Gao Xin District, 163319 Daqing Heilongjiang, China. E-mail: shijiamin0519@163.com
[2] Faculty of Agricultural Engineering and Information Technology, Heilongjiang Bayi Agricultural University, 5 Xin Feng Street Gao Xin District, 163319 Daqing Heilongjiang, China. E-mail: wixuexi444@gmail.com
[4] *Faculty of Information and Electrical Engineering, Heilongjiang Bayi Agricultural University, 5 Xin Feng Street Gao Xin District, 163319 Daqing Heilongjiang, China. E-mail: 7283022@qq.com

the operation of the ground wheel slippage and chain jump phenomenon, resulting in varying degrees of leakage of seeding problems [2], the design and development of an electric drive seed dispenser control system in line with the characteristics of the terrain of the Heilongjiang River and the performance of stable and reliable is so necessary [3]. With the continuous innovation of sensor technology, control algorithms and other aspects, intelligent control technology is widely used in the field of agricultural production. In the process of seed discharge, electric drive operation is gradually applied, the motor as a power source, can effectively shield the ground conditions and other external factors interference, through the electric drive seed discharge to realize efficient operation has become an effective program, at the same time, scholars at home and abroad for the electric drive control to carry out a lot of research. Kamgar et al [4] designed a seeding controller to obtain the desired seeding rate at different forward speeds and presence of stubble in grain strip planters. The electric drive system studied by Cay et al [5-6] combines PWM and PID techniques to better achieve the recommended optimum seeding rate, and the system was used in real operations to test the system, which performed better than the classical control system. Zhang et al [7] designed an electronically controlled corn seeding system, which showed good working performance during field sowing operation, and could quickly reach the target seeding rotation speed and improve the seeding precision. Ren et al. [8] designed a DC brushless motor control system based on a sliding film variable structure for an air-aspirated corn seeder, which realized precise control of speed and seeding volume.

Aiming at the above problems, this paper takes the seed discharger as the research object and designs the seed dispenser drive and control system suitable for complex terrain. In order to realize the above functions, this design adopts a DC brushless motor to drive the work of the seeder, and develops the supporting functional circuits based on the theoretical knowledge of the principle of motor control and joins the fuzzy PID control algorithm. Through the PID control parameter adjustment test, the adjustment enhances the precision and stability of the control system.

In order to test and verify that the research-designed electric drive seed discharger control system is functionally sound and complete and can demonstrate the superiority of electric drive control, the speed accuracy test of the seed discharger, the seeding performance test and the field test are conducted.Taking the grain spacing qualification index, standard deviation and coefficient of variation as test indexes, field tests were carried out to verify the working performance of the control system of the electric drive seed discharger.

2 Overall Design of the Electric Drive Control System

The electric drive seed expeller control system consists of a DC brushless motor driver, a power supply, a Hall encoder, a DC brushless motor, an air suction

seed expeller and other components. The motor drive uses STM32F103C8T6 as the core controller. During the seeding operation, the controller calculates the rotational speed to be achieved by the seeder according to the received information about the travel speed of the planter and the set plant spacing, and then feeds it back to the driver for the accurate control of the brushless DC motor. Among them, STM32 microcontroller is the core part of the control system, the main function is to provide the host computer with the current work of the actual rotational speed and row of seed quality information, and the second is to receive and parse the instructions issued by the host computer and perform the corresponding operation [9].

The motor control adopts a double closed-loop control structure, where the inner loop can track and regulate the motor speed in real time, and the outer loop controls the output of the inner loop. This hierarchical structure makes the system more resistant to external disturbances and parameter changes [10], improves the robustness of the system, and enhances the system response speed and stability [11]. The motor speed is calculated by monitoring the motor rotor position parameter changes through Hall sensors, and the speed is adjusted in real time according to the speed deviation and deviation rate of change, and a fuzzy PID algorithm is added to implement the speed control command to optimize the proportional-integral-derivative parameters, and the fuzzy control is introduced, so that the system responds to deal with the complex conditions with more excellent processing. The control system structure is shown in Fig. 1.

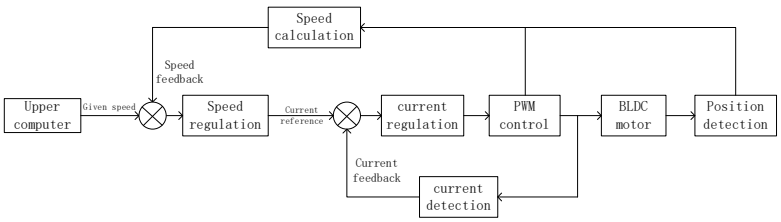

Fig. 1 Control system structure

3 Hardware Circuitry Design

The hardware circuit of this driver includes power supply circuit, STM32 core control circuit, motor drive circuit, serial debugging circuit, CAN communication circuit and other functional circuits. This paper mainly focuses on the power supply circuit, motor drive circuit to do the main introduction.

3.1 Power circuit module

In the actual field operation, seeder can be supplied with 12.0V DC power supply. The normal operating voltage of the main control circuit module is about 3.3V, and the voltage required for communication and motor drive modules is supplied at about 5.0V. Because the battery can not be directly to its power supply,

so build a step-down power supply circuit to ensure that the normal operation of each module operation, the schematic diagram shown in Figure 2.

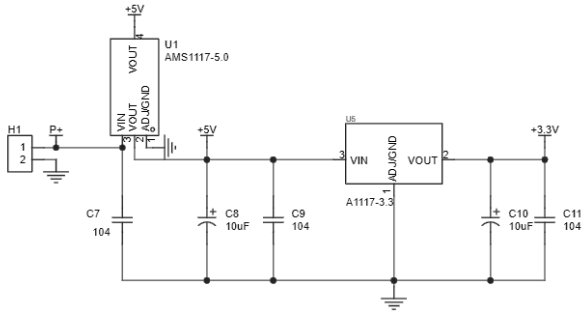

Fig. 2 Schematic diagram of power supply circuit

A 12.0V input voltage can be converted to a 5.0V input voltage using the AMS1117-5.0 forward low dropout regulator. The circuit is capable of converting an unstable input voltage to a stable 5.0V. The chip input voltage range is relatively wide, usually in the 6.0V to 15.0V, and has an overcurrent protection and overheating protection, resistance to extreme cold and high temperature, can be very good to meet the operating environment of the northeastern region [12]. The AMS1117-3.3 voltage regulator chip is used to convert the 5.0V power supply into 3.3V power supply for the microcontroller.

3.2 Drive motor circuit module

Suitable for complex operating environments motor drive phase change circuit design shown in Figure 3, the circuit for the three-phase in the U-phase circuit, the other two-phase circuit V, W and its same. The circuit uses the IRS2101SPBF driver with a three-phase full-bridge inverter circuit, and the DC brushless motor control method is currently usually used to convert the input signal into a pulse width modulation(PWM) signal to control the on-state and off-state of the switching tubes [13], so as to accurately control and regulate the circuit, and to realize the speed regulation of the motor.

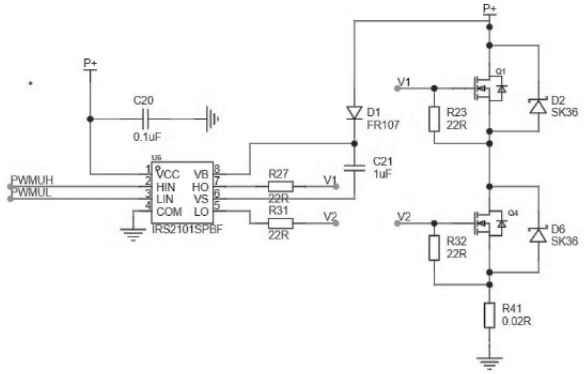

Fig. 3 Motor Drive Phase Change Circuit

The IRS2101PBF operates from 10V to 20V, with the VCC pin connected to a 12V supply; the input P+ is connected to a bootstrap capacitor, which is charged by a diode to the bootstrap capacitor, whose stored energy is used to ensure the stable on-state operation of the MOSFETs, and a bypass capacitor is connected to ground. The microcontroller transmits the generated PWM signals to the HIN and LIN pins through an optocoupler isolation circuit [14], and then to the MOSFET via the HO and LO pins to control its turn-off. The resistor in parallel with the MOS tube is its pull-down resistor, which serves to prevent breakdown of the MOS tube due to the absence of a charge release loop under electrostatic action, and also prevents the tube from being burned out by the uncontrolled drain current generated during power-up [15]. In order to make the MOS tube can be shut down quickly, a continuity diode is connected in parallel next to it. This circuit can provide enough drive current for the DC brushless motor and can independently and stably control the DC brushless motor operating state.

4 Control Algorithms and Simulation Experiments

4.1 Mathematical modeling of DC brushless motor

Mathematical modeling of the DC brushless motor [16], for use in subsequent control system simulation, the state change and electrical characteristics of the motor mathematical model and the actual platoon motor can be better approximated [17], which can better simulate the performance of the DC brushless motor and make the experimental results more accurate. The three-phase balance equation for a brushless DC motor is

$$\begin{bmatrix} U_a \\ U_b \\ U_c \end{bmatrix} = \begin{bmatrix} r & 0 & 0 \\ 0 & r & 0 \\ 0 & 0 & r \end{bmatrix} \begin{bmatrix} i_a \\ i_b \\ i_c \end{bmatrix} + \begin{bmatrix} L-M & 0 & 0 \\ 0 & L-M & 0 \\ 0 & 0 & L-M \end{bmatrix} P \begin{bmatrix} i_a \\ i_b \\ i_c \end{bmatrix} + \begin{bmatrix} e_a \\ e_b \\ e_c \end{bmatrix} \quad (1)$$

Where:

U_a, U_b, U_c…Three-phase winding terminal voltage [V],

i_a, i_b, i_c…Three-phase winding phase current [A],

r…Resistance per phase of winding [Ω],

L…Self-inductance per phase of winding [H],

M…Mutual inductance between the windings of each two phases [H],

P…Differential operator, P=d/dt [-].

The DC brushless motor electromagnetic torque equation is

$$\boldsymbol{T_e} = \frac{\boldsymbol{e_a i_a + e_b i_b + e_c i_c}}{\boldsymbol{w}} \quad (2)$$

Where:

T_e…Electromagnetic torque [N·m],

w…Motor rotor mechanical speed [rad/s^2].

The mechanical equation of motion of a brushless DC motor is

$$\boldsymbol{T_e - T_l - Bw = J\frac{dw}{dt}} \tag{3}$$

Where:

T_l…Load torque [N·m],
J…moment of inertia (mechanics) [kg·m2],
B…Damping factor [-].

4.2 Fuzzy PID control algorithm design

The DC brushless motor is a nonlinear system, and the traditional PID control algorithm is a linear model-based control method, which has poor adaptability and insufficient robustness to the nonlinear system, and the control effect is limited. The gain-tuned fuzzy PID algorithm [18] is currently more commonly used, and in this paper, an improved fuzzy PID control algorithm is used, which combines the advantages of fuzzy logic, and is able to better cope with the nonlinear characteristics in the motor system.

In practical operations, firstly, the obtained rotational speed deviation e and the rate of change of deviation e_c as inputs to the actual control quantities are quantized and fuzzified to correspond with the fuzzy theoretical domain to obtain E and E_c, and the affiliation function is determined in order to be able to take into account the ambiguity and uncertainty of the system [19]. Commonly used affiliation functions are triangular, trapezoidal, and Gaussian [20], of which the triangular affiliation function is more intuitive and flexible for experimental observation. For input variables at any time, the degree of affiliation belonging to a fuzzy set can be calculated by the affiliation function and thus converted to a fuzzy variable.

Next, fuzzy inference is performed using the expert knowledge from the already established fuzzy rule base. First find the affiliation degree $\mu_{k_{p(j)}}$, $\mu_{k_{i(j)}}$, $\mu_{k_{d(j)}}$ of the jth ($j = 1,2 \cdots ,49$th)fuzzy rule corresponding to $\Delta k_p, \Delta k_i, \Delta k_d$ [21]. The fuzzy outputs are derived through fuzzy logic operations, where the fuzzy subsets of the input and output fuzzy variables are defined as {Positive Big (PB), Positive Medium (PM), Positive Small (PS), Zero (ZE), Negative Small (NS), Negative Medium (NM), Negative Big (NB)} [22]. When performing fuzzification, the input variables shall be converted from the fundamental domain to the corresponding fuzzy sets. In this process, the input variables shall be multiplied by the corresponding quantification factors. The quantification factor is denoted by K. The error quantization factor K_e and the quantization factor of error change K_{ec} are obtained from the following two equations.

$$\boldsymbol{K_e = \frac{n_e}{E}} \tag{4}$$

$$\boldsymbol{K_{ec} = \frac{n_e}{E_c}} \tag{5}$$

Setting the domain of each variable as [-6, 6], Figure 4 shows the triangular affiliation function of the input variable e and the output variable Δk_p.

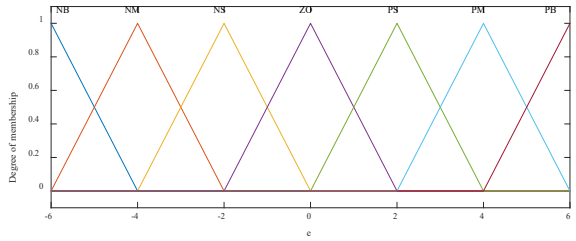

Fig. 4(a) Input variable e triangular affiliation function

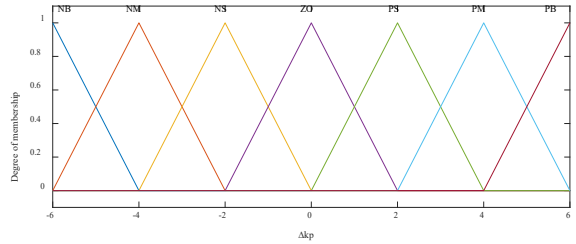

Fig. 4(b) The output variable Δkp triangular affiliation function

Finally, the fuzzy outputs are converted into specific control quantities Δk_p, Δk_i, and Δk_d by defuzzification and input to the PID controller for control parameter tuning in order to achieve precise control of the system.

$$\Delta \boldsymbol{k_p} = \frac{\sum_{j=1}^{49}\left\{\mu_{k_{p(j)}\Delta k_p(j)}\right\}}{\sum_{j=1}^{49}\mu_{k_{p(j)}}} \tag{6}$$

$$\Delta \boldsymbol{k_i} = \frac{\sum_{j=1}^{49}\left\{\mu_{k_{i(j)}\Delta k_i(j)}\right\}}{\sum_{j=1}^{49}\mu_{k_{p(j)}}} \tag{7}$$

$$\Delta \boldsymbol{k_d} = \frac{\sum_{j=1}^{49}\left\{\mu_{k_{p(j)}\Delta k_p(j)}\right\}}{\sum_{j=1}^{49}\mu_{k_{p(j)}}} \tag{8}$$

Using the rectified PID parameters Δk_p, Δk_i and Δk_d, the relationship between input $e(t)$ and output $u(t)$ is determined as in equation (9).

$$\boldsymbol{u(t) = \Delta k_p e(t) + \Delta k_i \int_0^t e(t)dt + \Delta k_d \frac{de(t)}{dt}} \tag{9}$$

4.3 Control system simulation model construction and simulation experiment

According to the analysis and design of the DC brushless motor control principle, the fuzzy PID-based DC brushless motor control system is established by using the Simulink toolbox in MATLAB, as shown in Fig. 5, and the modules of

the simulation system mainly include the motor overall module, speed control module, current control module, inverter module and other auxiliary modules.

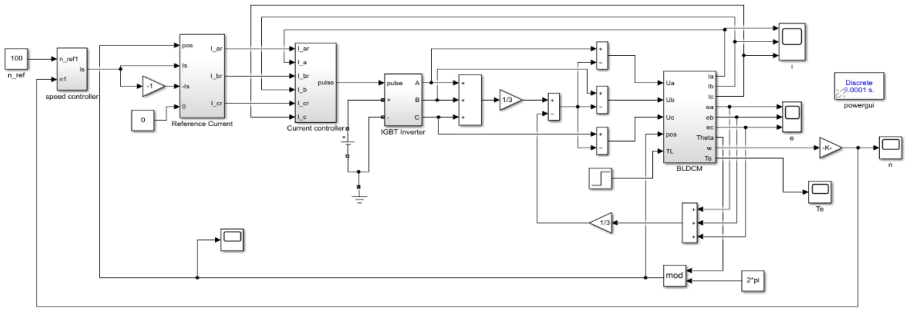

Fig. 5 Block diagram of fuzzy PID-based DC brushless motor control system

The fuzzy PID algorithm is applied to the speed control module, whose input is the error variable of the speed and the output is the actual three-phase current value, which is used as the input reference value of the current regulation module. The current control module adopts the hysteresis loop control strategy to compare the actual current value with the reference current value to obtain the switching tube control signal. The overall module of DC brushless motor includes DC brushless body module, torque equation module and kinematics equation module, and each module is constructed according to the above established mathematical model of the motor as a theoretical basis, in which the inputs of the body module are the rotor position signals, three-phase terminal voltages, and angular velocities, and the outputs are the three-phase currents and the numerical values of the inverse electromotive force, and a segmented linear method is adopted in obtaining the three-phase inverse electromotive force, and an S-function is written to complete the modeling of the inverse electromotive force.

Based on the above theoretical foundation and the constructed simulation model, analysis and simulation are carried out. The parameters of the DC brushless motor are set as follows: stator armature winding resistance R=1Ω in each phase; self-inductance of stator armature winding and mutual inductance difference between windings L-M=0.081H in each phase; rotational moment of inertia J=0.005 Kg·m2; differential operator P=1. The system load is started, the load torque T_L=1N·m, the set rotational speed n=100 r/min, and the system simulation time is set to 1s. Fig. 6 and Fig. 7 show the three-phase current and three-phase opposite electromotive force waveforms of the simulation of the control system of the DC brushless motor.

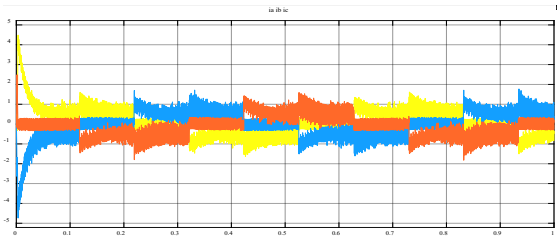

Fig. 6 Three-phase current waveform

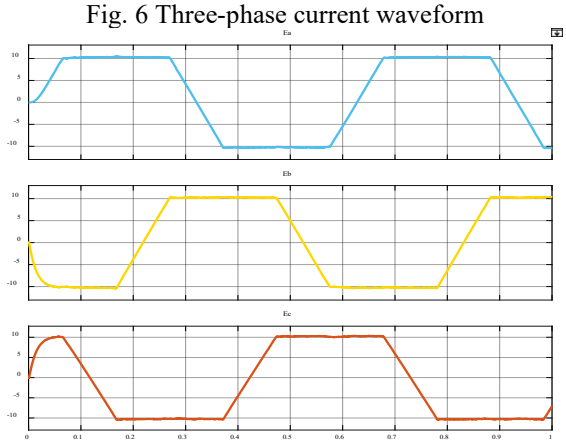

Fig. 7 Three opposite electromotive force waveforms

From the stator three-phase current waveforms, it can be seen that the initial start-up current is large, but in a very short time to enter a stable state, each phase of the current according to a reasonable waveform to work. From the stator winding three opposite potential waveforms, it can be seen that the value of each opposite electromotive force is stable in accordance with the established three-phase equilibrium equation operation, the system began to simulate, A opposite electromotive force from 0 began to rise in a very short time to reach the top of the wave and the set value of the reverse electromotive force smoothly.

Figure 8 shows the rotational speed waveform, it can be seen that the speed from 0 to about 100 r/min adjustment time is 0.1s, no overshooting and no obvious oscillation after reaching the steady state, it can be seen that the system stability is good.

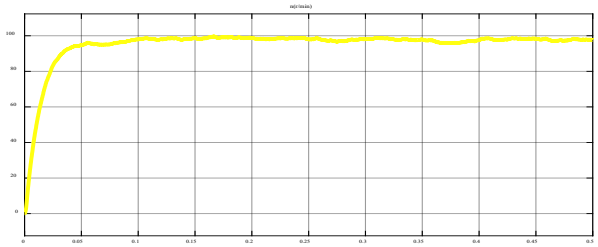

Fig. 8 RPM Waveform

5 Performance Testing and Field Trials

5.1 System response time detection test

There is a certain response delay in the work of air-absorbent planter motor-driven seed discharger, and this delay has less impact when the planter is running at uniform speed, but it can lead to a reduction in the seeding pass rate during accelerated start and decelerated stop. When accelerating start, the axial movement of the motor lags behind the movement of the machine, which may lead to an increase in the leakage rate; while when decelerating and stopping, the response time of the motor may lead to an increase in the reseeding rate, which in turn affects the seeding pass rate. Therefore, analyzing and detecting the response time plays an important role in optimizing the control system.

The test was conducted using a Gwinstek-6050 oscilloscope, and the XD-37GB3650 brushless DC motor was passed through a pulse generator, which outputs +5V pulses varying with the rotational speed from the signal line, and the output sends out a positive-to-negative voltage signal for every one-week rotation of the drive motor. Figure 9 shows the output pulse waveform, where the oscilloscope parameters are adjusted to 2ms/unit for the X-axis and 2V/unit for the Y-axis.

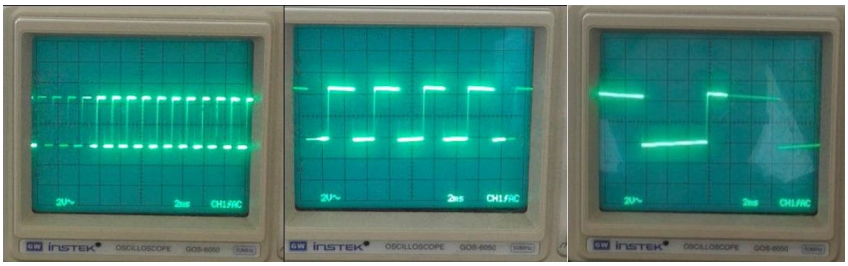

a: Waveform at 500r/min, b: Waveform at 240r/min, c: Waveform at 100r/min

Fig. 9 XD-37GB3650 DC permanent brushless motor output pulse waveforms

In the actual test, the Debonair Dawei 2BGM-2 2-row pneumatic suction no-till corn planter was used, and the traction equipment was a John Deere 6B-1404 farm tractor. During the test, the tractor was selected to run smoothly for 3s-5s after accelerating to 12km/h from a standstill, then decelerating smoothly to a standstill, and the response time of the electric drive seeder system was measured under the conditions of acceleration, uniform speed and deceleration.

The experimental results are shown in Fig. 10, in which the green data line represents the current rotational speed of the seed dispenser drive motor, which is used to obtain the seed dispenser rotational speed information by generating a pulse signal for every revolution of the motor and collecting the number of pulses in 1 second. The red data line represents the current forward speed signal of the tractor, which is in the range of 0km/h to 15km/h and is sent through the upper computer. For comparison with the motor speed signal, the speed signal is multiplied by a

factor of 26 to ensure that the tractor forward speed signal varies between 0 and 390. This allows for a comparative experimental study between tractor forward speed and drive motor speed.

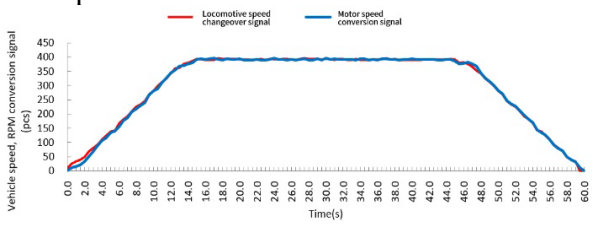

Fig. 10 Response curves for different conditions of electrically driven seed dischargers

The vehicle speed and speed conversion signals in Fig. 10 are differenced to calculate the relative percentage between the vehicle speed and the speed of the seed discharger, and the difference is shown in Table 1.

Table 1

Data table of relative deviation of motor speed signal and tractor signal

Time t(s)	Tractor operating status	Maximum percentage deviation of motor speed from tractor running speed (%)
0-15s	The tractor is up and running.	-80.00%~+57.69%
3.5-15s	Tractor speeding up	-1.66%~+7.20%
15-45s	Tractor running at constant speed	-1.50%~+1.79%
45-60s	Tractor decelerates to a stop	-4.55%~+6.06%

As can be seen from the above table, the overall look of the electric drive seed dispenser in the start-up phase there is a large deviation, in the uniform speed and deceleration process speed signal shows good followability, the tractor speed conversion signal and the motor speed signal between the fit is high. It can be seen that the overall stability and followability of the electric drive seed dispenser control system is good, and can better meet the actual production requirements.

5.2 Field trials

The test selected Tiannong No. 9 corn seed, according to its sowing requirements, using Debang Dawei 2 rows of 2BGM-2 pneumatic suction no-tillage planter as the test object, the seeder is shown in Figure 11.

a: Photo of the planter, b: Seeding experiment
Fig. 11 Electrically driven seed dischargers tester

Set the sowing plant spacing of 25 cm, row spacing of 65 cm, the traction tractor forward speed were selected to run at low (4 km/h), medium (8 km/h), high-speed (12 km/h) speed, respectively, to test the mechanically driven sowing and the electric drive planter seeding grain spacing qualifying indexes, the standard deviation and the coefficient of variation of the three indexes to compare the two modes of operation of the sowing qualifying rate, and thus to validate the reliability of the electric drive row seeding control system. The statistics of seeding parameters of tractor at 4 km/h, 8 km/h, 12 km/h are shown in Table 2.

Table 2

Statistics of tractor seeding parameters at 4km/h, 8km/h and 12km/h

Statistical parameters	Tractor operation 4 km/h		Tractor operation 8 km/h		Tractor operation 12 km/h	
	Electric seed dispenser	Mechanically driven seed dispenser	Electric seed dispenser	Mechanically driven seed dispenser	Electric seed dispenser	Mechanically driven seed dispenser
Maximum distance(cm)	33.4	29.8	28.6	30.3	30.1	44.7
Minimum distance(cm)	18.8	21.1	20.3	19.5	17.9	13.5
Average distance $\bar{L}$(cm)	25.3	25.1	25.1	25.3	24.5	26.2
Standard deviation S(cm)	2.651	1.861	1.489	1.974	2.211	5.877
Variation coefficient L	10.48%	7.45%	6.11%	7.91%	8.91%	22.23%

From the measured results and data analysis, it can be seen that the measured values of seeding spacing of the electrically driven seeder at low, medium and high speeds were in the range of 17.9 cm-33.4 cm, during which there was no monitoring of the occurrence of leakage by reseeding, while the measured values of seeding spacing of the mechanically driven seeder under the same operating conditions were

in the range of 13.5 cm-44.7 cm, during which there was monitoring of one leakage and no reseeding.

It can be seen that at low speeds, the standard deviation distribution of the mechanical seeder is slightly lower than that of the electric-driven rower, which performs relatively well; at medium speeds, the standard deviation distributions of the two modes are basically equal, and the sowing qualification rate is higher; whereas at high speeds, the electric-driven rower's sowing qualification rate is significantly higher than that of the ground-wheel-driven rower. The coefficient of variation (CV) for seeding at different speeds ranged from 6.11% to 10.48% for electrically driven seeders and from 7.45% to 22.23% for ground wheel driven seeders. In addition, the coefficient of variation of the ground-wheel-driven seeder showed an increasing trend with the increase of vehicle speed. Through the above data, it can be well reflected that under the high-speed running conditions, the electric-driven seeder shows better seeding pass rate, average spacing, standard deviation distribution and coefficient of variation compared with the ground-wheel-driven seeder, and it can comply with the technical standard of JB/T 10293-2013 single-grain (precision) seeder.

6 Conclusion

(1) A fuzzy PID control algorithm based on the electric drive seed dispenser control system is designed, and the Simulink simulation test shows that this control system has stable performance, fast response speed and small overshooting amount. Through the system response time test, it is tested that the system follows well and meets the demand of the control program.

(2) The field test showed that the performance of mechanically driven seed expeller and electrically driven seed expeller was compared at a sowing spacing of 25cm. Under the three operating speeds of low speed (4 km/h), medium speed (8 km/h) and high speed (12 km/h), the electrically-driven seed spreader is better than the mechanically-driven seed spreader in terms of spacing qualification index, standard deviation and coefficient of variation, and the leakage rate and replanting rate are all reduced. The results of the study were able to make sowing less discrete compared to the set theoretical spacing values, thus ensuring uniform spacing and consistent number of seeds to improve seed viability, germination and hence crop yield.

This electric drive control system, based on the fuzzy PID algorithm, has a good coping ability for the multicasting and omission of seeding, which are easy to occur in the operation. It realizes high-quality precision sowing of crops, improves the accuracy and stability of agricultural machinery and equipment, and increases the efficiency and sustainability of agricultural production.

REFERENCES

[1] *Zhou, M*. Exploring the advantages of green development and food security issues in Heilongjiang. Grain Science and Economy, 2020, 45(11):40-41.

[2] *Sui, B., Zhang, Q.D., Zhang, Z.Y*. On agricultural engineering science and technology innovation in the context of rural revitalization strategy. Journal of Agricultural Engineering, 2019, 35(4):1-10.

[3] *Hou, Y.T*. Research and development of high-speed precision seeding technology with electric drive. China Agricultural Digest-Agricultural Engineering, 2023, 35(04):7-11.

[4] *Kamgar S, Noei-Khodabadi F, Shafaei S M*. Design, development and field assessment of a controlled seed metering unit to be used in grain drills for direct seeding of wheat. Information Processing in Agriculture, 2015, 2 (3-4);11-14

[5] *Cay A, Kocabiyik H, May S.* Development of an electro-mechanic control system for seed-metering unit of single seed corn planters Part II: Field performance. Computers and Electronics in Agriculture, 2018, 145: 11-17.

[6] *Cay A, Kocabiyik H, May S.* Development of an electro-mechanic control system for seed-metering unit of single seed corn planters Part I: Design and laboratory simulation. Computers and Electronics in Agriculture, 2018, 144: 71-79.

[7] *Zhang, C.L., Wu, R., Chen, L.Q*. Design and test of electronically controlled corn seed discharge system. Journal of Agricultural Machinery, 2017,48(02):51-59.

[8] *Ren, S.H., Yi, S.J.* Control Mechanism and Experimental Study on Electric Drive Seed Metering Device of Air Sunction Seeder. Tehnicki Vjesnik-Technicalngazette, 2022, 29(4), 1254-1261.

[9] *Yang, L., Yan, B.X., Zhang, D.X. et al*. Research progress of precision sowing technology for corn. Journal of Agricultural Machinery, 2016,47(11):38-48.

[10] *Gao, T.J., Z, B., Yi, S.j. et al.* Research on sowing metering monitoring system of precision planter. Agricultural Mechanization Research, 2016,38(12):96-100+106.

[11] *Zhao, X.S., Ran, W.J., Yan, Q. et al*. Design and test of electronically controlled seeding system. Agricultural Mechanization Research, 2022,44(02):67-73.

[12] *Guo, H.L., Zhao, Y.H., Li, M.W. et al.* Design of intelligent seeding control system based on BLDCM. Agricultural Mechanization Research, 2019, 41(02): 201-205+210.

[13] *Yan, Q.* Design and experimental research of electronically controlled seed discharge system. Hebei Agricultural University, 2020.

[14] *Ding, Y.Q., Yang, L., Zhang, D.X. et al.* Design of Monoblock drive for corn variable planter. Journal of Agricultural Engineering, 2019,35(11):1-9.

[15] *Zhu, J.J., Liu J., Fu Y.B. et al*. Design and test of control system for grain precision seed discharge. Agricultural Mechanization Research, 2022, 44(09): 89-93+98.

[16] *Jafari M, Hemmat A, Sadeghi M*. Development and performance assessment of a DC electric variable-rate controller for use on grain drills. Computers and Electronics in Agriculture, 2010, 73 (1);12-15.

[17] *Dang, X*. Research on brushless DC motor control system based on STM32. Anhui University of Technology, 2018.

[18] *Yao, Y.F., Chen, X.G., Ji, C. et al*. Design and test of monoblock drive for corn precision planter based on fuzzy PID control. Journal of Agricultural Engineering, 2022,38(06):12-21.

[19] *Coelho, A.L.d.F., Queiroz, D.M.de, Valente, D.S.M., & Pinto,* F.A.C. (2020). Development of a Variable-Rate Controller for a Low-Cost Precision Planter. Applied Engineering in Agriculture, 36(2), 233–243.

[20] *Chen, L.Q., Xie, B.B., Li, Z.D. et al*. Design of corn precision seed discharge control system based on double closed-loop PID fuzzy algorithm. Journal of Agricultural Engineering, 2018,34(09):33-41.

[21] *Wang, S., Zhao, B., YI, S.J. et al.* Research on control system of electric mung bean planter based on IGWO-LADRC. Journal of Agricultural Machinery, 2022,53(S1):87-98.

[22] *Zhao, X.S., Zhao, D.W., Yan, Q. et al*. Fuzzy PID-based electronically controlled precision seeding system and experimental research. Journal of Hebei Agricultural University, 2021,44(01):120-127.